Journal of Diabetes Science and Technology
Volume 7, Issue 2, March 2013

TECHNOLOGY REPORT

A Promising Solution to Enhance the Sensocompatibility of Biosensors in Continuous Glucose Monitoring Systems

Edith E. M. van den Bosch, Ph.D., Nik H. M. de Bont, B.Sc., Jun Qiu, Ph.D., and Onko-Jan Gelling, Ph.D.

Abstract

Background:

Continuous glucose monitors (CGMs) measure glucose in real time, making it possible to improve glycemic control. A promising technique involves glucose sensors implanted in subcutaneous tissue measuring glucose concentration in interstitial fluid. A major drawback of this technique is sensor bioinstability, which can lead to unpredictable drift and reproducibility. The bioinstability is partly due to sensor design but is also affected by naturally occurring subcutaneous inflammations. Applying a nonbiofouling coating to the sensor membrane could be a means to enhancing sensocompatibility.

Methods:

This study evaluates the suitability of a polyethylene-glycol-based coating on sensors in CGMs. Methods used include cross hatch, wet paper rub, paper double rub, bending, hydrophilicity, protein adsorption, biocompatibility, hemocompatibility, and glucose/oxygen permeability testing.

Results:

Results demonstrate that coating homogeneity, adhesion, integrity, and scratch resistance are good. The coating repels lysozyme and bovine serum albumin, and only a low level of fibrin and blood platelet adsorption to the coating was recorded when testing in whole human blood. Cytotoxicity, irritation, sensitization, and hemolysis were assessed, and levels suggested good biocompatibility of the coating in subcutaneous tissue. Finally, it was shown that the coating can be applied to cellulose acetate membranes of different porosity without changing their permeability for glucose and oxygen.

Conclusions:

These results suggest that the mechanical properties of the coating are sufficient for the given application, that the coating is effective in preventing protein adsorption and blood clot formation on the sensor surface, and that the coating can be applied to membranes without hindering their glucose and oxygen transport.

J Diabetes Sci Technol 2013;7(2):455–464

Author Affiliation: DSM Biomedical, Geleen, The Netherlands

Abbreviations: (BSA) bovine serum albumin, (CGM) continuous glucose monitor, (NaCl) sodium chloride, (PBS) phosphate-buffered saline, (PEG) polyethylene glycol, (PET) polyethylene terephthalate, (SMBG) self-measurement of blood glucose, (UV) ultraviolet

Keywords: biocompatibility, biofouling, coating, continuous glucose monitoring, glucose sensor

Corresponding Author: Edith E. M. van den Bosch, Ph.D., DSM Biomedical, Koestraat 1, 6167 RA Geleen, The Netherlands; email address *edith.bosch-van-den@dsm.com*

Introduction

Strict glycemic control is a major concern in people with diabetes.[1–3] The use of systems for self-measurement of blood glucose (SMBG) or glucose meters helps patients with diabetes obtain better glycemic control through monitoring of blood glucose levels several times a day. Continuous glucose monitors (CGMs) measure glucose in real time and can predict future trends.[4] This offers the potential to predict hypoglycemic events and describe patterns of glucose variability that may not be detectable from SMBG devices. Different noninvasive techniques have been developed to obtain continuous glucose measurements.[5–10] In general, invasive techniques seem to be superior to noninvasive techniques because of better accuracy and reduced lag time of glucose measurements.[5,9] One of the most promising invasive techniques involves the implantation of a glucose sensor in subcutaneous tissue.

Typically, such a system consists of multiple elements, including a subcutaneous glucose sensor that is worn for a few days and then replaced, a link from the sensor to a nonimplanted transmitter that communicates to a receiver, and an electronic receiver worn like a pager that displays continuous glucose level updates. Unlike SMBG devices that sample glucose levels from capillary, arterial, or venous blood, CGMs measure the glucose concentration in the interstitial fluid just under the skin.

The CGM sensor is, in most cases, composed of a plastic support with an electrode that carries an enzyme matrix and is covered by a membrane layer. The membrane layer acts as a barrier between the electrode on the sensor and its surroundings. Current commercially available CGM sensors draw their readings from the glucose-oxidase-catalyzed oxidation of glucose by oxygen. In this chemical reaction, hydrogen peroxide is generated, which then reacts further to generate an electric current that can be measured with electrodes.[11,12] One important aspect of the membrane used in CGMs is adequate glucose and oxygen permeability.

A major drawback of subcutaneously implanted electrochemical sensors is their bioinstability, which can lead to unpredictable drift and reproducibility of sensor measurements.[13–17] As a result, the sensor must be calibrated with a traditional blood glucose measurement, and it is advised to use capillary stick measurements to confirm hypoglycemia or hyperglycemia before taking corrective action.[18] The bioinstability is explained by the sensor design and/or subcutaneous inflammatory reactions. Suggested causes of bioinstability are biofouling in or on the membrane, tissue interferents affecting the electrode, enzymatic dysfunction, and unstable levels of oxygen.[19–23] Once implanted, a sensor membrane becomes covered with plasma proteins as a result of increased vascular permeability and/or disrupted vessels where fibrinogen causes inflammation.[24–28] In chronic stages, the implant is walled off by granulation tissue, and eventually, a fibrous capsule is formed.[29] In addition, tissue hemorrhage and resulting blood clots near a sensor can result in lowered local blood glucose concentration and inaccurate readings due to metabolic reactions. Tissue hemorrhage and associated accumulation of metabolically active red blood cells near the CGM sensor are common and occur as a result of sensor movement within the subcutaneous tissue. Research shows that sensor signal is lost when a blood clot comes into direct contact with the electrode surface. Fibrin clots seem to be important in maintaining red blood cells that are in close contact with the sensor.[30] A potential strategy to reduce tissue hemorrhage and local inflammation is the inhibition of protein adsorption to the sensor surface by coating the outer membrane with a nonfouling coating. This report is the first study of DSM's VitroStealth® coating (Royal DSM N.V., Heerlen, The Netherlands).[31]

Methods

Coating Formulation

The coating formulation comprised silicon oxide nanoparticles containing polyethylene glycol (PEG) tails, an adhesion promoter, and a crosslinker.[31] When in contact with water, the PEG chains adopt a brush-like structure.

Silicon Wafer Activation

Prior to the coating application, the silicon wafer surface was activated with Piranha solution.

Silicon wafers (Siltronic AG; pieces 5 × 1 cm^2) were immersed in Piranha solution ($H_2O/H_2O_2/NH_3$; 5/1/1; v/v/v) and heated at 50 °C for 15 min. After activation, the wafers were rinsed with and stored in distilled water for a maximum of two days. The coating was applied immediately after the wafers were dried with pressured air.

Spin Coating

Spin coating and ultraviolet (UV) curing were used to apply the coating to the activated silicon wafers.

A wafer was positioned at the center of the spin coater plate (Convac ST146 spin coater), and filtered (0.25 μm cellulose filter) coating formulation (2 w% solids) was applied. The formulation fully covered the wafer surface. Excess formulation was removed by rotating the silicon wafer at 1800 rpms for 10 s. Coatings were applied at 19–22 °C at a relative humidity below 55%. Coated samples were stored in air for 5 min prior to UV curing. Curing was performed in a UV rig containing a VPS/I600 system from Fusion UV systems Inc.® with D-bulb at a dose of approximately 2 J/cm^2, under nitrogen and at a conveyor speed of 18 m/min.

Mayer-Bar Coating

Mayer-bar coating and UV curing were used to apply the coating to polyethylene terephthalate (PET) sheets.

Coating formulation (7 w% solids) was applied to 188 μm thick PET sheets (Toyobo; cleaned with ethanol-soaked VWR Spec-wipe® 115-0036 tissues) by means of a size 0 roll bar. Coated samples were air dried for 5 min prior to UV curing (discussed earlier).

Membrane Coating

Cellulose acetate membrane filters (Sterlitech) were immersed in the coating formulation for 2 min under gentle stirring. Immediately afterward, they were placed on a Buchner funnel with the small pore side facing down. A filter paper (Machery Nagel MN 640) washed in methanol was placed between the funnel and the membrane. After a 30 ml coating formulation was poured into the funnel, a vacuum was applied to achieve a drawing force of 950 mbar. Total suction time was 3 min. The filter was then removed from the funnel and allowed to dry at room temperature for 1 h. Ultraviolet curing was performed as described earlier.

Polyethylene Terephthalate Tube Coating

Prior to the coating application, PET tubes (GreinerBio-One) were washed with methanol, rinsed with distilled water, and air dried.

Subsequently, the tube was filled with the coating formulation (7 w% solids), and the formulation was aspirated at a constant speed via a thin steel needle. After the bulk formulation was withdrawn, needle suction continued for an additional 10 s to ensure the removal of residual coating formulation. The coating was subsequently air dried for 5 min and UV cured (2 J/cm^2) by means of a Macam Flexicure Controller with light-guide (UVL5101-8 2102).

Coating Thickness Determination

Uncoated and coated PET sheets were subsequently mounted on a sample holder perpendicular to a regulated tungsten halogen light source in Filmetrics F-20 equipment. The amount of light reflected was measured over a range of wavelengths for both sheets. Differences in the recorded reflectance spectra were used to calculate coating thickness.

Determination of Coating Defects

Coated PET sheets were held against light at a distance of 20–25 cm from the eyes. The sheets were subsequently rotated from 90° to 0° until a rainbow or purple–blue reflection was observed. Variations in coating thickness result in different light reflections, and thus different colors were observed. Further visual inspection was performed using optical light microscopy at a magnification of 100× to detect micrometer size defects.

Cross-Hatching Test (ASTM D3002 –D3359)

Using a pattern knife, lattice patterns were cut through the coating on the PET sheet. Next, the coating surface was brushed using a diagonal motion to remove cutting dust. Scotch tape was forcefully applied to the lattice pattern on the coating and then removed, eliminating trapped gas bubbles. Subsequently, the scotch tape and coating surfaces were visually inspected. In this method, coatings were classified in six categories, ranging from ASTM Class 5B (the edges of the cuts were smooth, none of the lattice squares were detached) to Class 0B (the coating completely flaked off from the substrate).

Wet Paper Rubbing Test

Strips (2.3 × 12 cm^2) of coated PET film were wetted with distilled water for 5 s. The film was then placed on a flat surface and covered with (water) prewetted papers (2.6 × 4.7 cm^2). On the pile of wet papers, 550 g of force was applied by placing a glass bottle filled with water on top of it (approximately 1.1 bar effective pressure). Subsequently, the papers and the glass were moved back and forth 10 times. After rinsing the coated film with distilled water for approximately 5 s, coating cohesion and adhesion between the coating and the substrate were evaluated by visual inspection.

Paper Double Rubbing Test

A dry paper tissue was placed on top of the coated PET film and manually circulated six times on a coating surface area of 1 × 4 cm^2. The area was then visually inspected for scratches and coating removal.

Bending Test (ASTM E290-09)

Coated substrates were bent around a pencil to evaluate the coating for crack formation, which indicates coating flexibility.

Evaluation of Hydrophilicity

In order to verify the hydrophilicity of the coated substrate, wetting behavior of the coated substrate was evaluated.

A total of 10 μl of distilled water was applied to a coated flat substrate and given a dwelling time of 5 s. Wetting behavior was recorded as the diameter of the circle formation.

Lysozyme Adsorption Test

Hen egg white lysozyme was purchased from Sigma and used without further purification. A 160 ppm lysozyme solution was prepared in 10 mM potassium phosphate buffer. Fresh lysozyme solution was used for each instance of adsorption testing.

Initially, samples were immersed in the phosphate buffer for 1 h to allow swelling. Subsequently, lysozyme adsorption on coated silicon wafers was measured by using stagnation point flow reflectometry. The change in intensity of the reflected polarized He–Ne laser, which was caused by lysozyme adsorption on the spin-coated silicon wafer, was converted into adsorbed mass using a matrix model.[32] After introducing the buffer to the flow chamber for 5 min, the lysozyme solution was allowed to flow into the chamber. After observing a stable adsorption plateau for 2 min ("reversible protein adsorption"), the buffer was flushed through the chamber to replace the protein solution until a second plateau was reached ("irreversible protein adsorption").[31]

Bovine Serum Albumin Adsorption

Bovine serum albumin (BSA) adsorption to coated PET tubes was determined using [125I]-BSA (PerkinElmer). Several milliliters of protein solution were added to the tubes and incubated overnight in the dark and at room temperature. After aspiring the protein solution and washing the tubes with phosphate-buffered saline (PBS) solution (Dulbecco Biochrom AG) three times, the residual amount of radiation was determined using a liquid scintillation counter (PerkinElmer). The results were converted into a percentage of reduction in BSA adsorption as compared with the uncoated tubes.

Biocompatibility Testing

Sensitization, irritation, and hemolysis of the coating were evaluated (ISO 10993-1,10,4). In the sensitization test, coated PET sheets (120 cm^2) were separately extracted in 20 ml sodium chloride (NaCl) and cotton seed oil at 70°C for 24 h. After clipping the skin of the test sites of Hartley guinea pigs (35 animals) free of hair, intradermal injections of the pure extracts were made in the shoulder region (induction phase). On day 6, animals that showed no signs of irritation or corrosion after the induction application were pretreated with 10% sodium dodecyl sulfate in petrolatum 24 h before the topical induction application. If irritation or corrosion was present, no pretreatment occurred. On day 7, pieces (2 × 4 cm^2) of extract-saturated filter paper were applied and left in place for 48 h. On day 23, pieces (2 × 2 cm^2) of extract-saturated filter paper were secured to previously unexposed areas of the animal (flank area) for 24 h. Immediately after removing the patches, the challenge sites were cleaned and shaved and examined at 24, 48 and 72 h after the challenge exposure period for signs of erythema and swelling. In the irritation test, the extracts were intracutaneously injected (0.2 ml per site) in New Zealand White rabbits (3 animals). The injection sites were observed for signs of erythema and edema immediately following injection and at 24, 48 and 72 h after injection. Observations conducted also included all clinical and toxicological signs. Hemolysis was evaluated using NaCl extracts of coated PET sheets (6 cm^2 per ml). Diluted fresh human blood was added to the extracts (0.2 ml per 10 ml). After incubation at 37°C for 60 min and centrifugation for 5 min at 750 × g, hemolysis was assessed by UV spectrophotometry of the supernatant at 545 nm.

Cytotoxicity was evaluated in the L929 minimum essential medium elution test and the systemic injection test (ISO 10993-5,11). Coated PET sheets (60 cm^2) were extracted in 10 ml complete minimum essential medium supplemented with 10% fetal bovine serum at 37°C for 24 h. Pure extract was used to replace the maintenance medium of a L929 cell monolayer >80% confluent. Microscopic evaluation of cellular reactivity was performed after incubation at 37°C for 48 h. In the systemic injection test, NaCl and cotton seed oil extracts of the coated PET sheets (discussed earlier) were respectively intravenously and intraperitoneally injected (50 ml per kg) in albino Swiss mice (20 animals). The animals were observed for clinical signs immediately after and at 4, 24, 48, and 72 h after injection.

Hemocompatibility Testing

Testing was performed by HaemoScan. Venous blood was collected from six donors who received no medication within 2 weeks preceding blood collection. A whole blood sample (60 ml) was drawn using heparin (1.5 IU/ml) as anticoagulant. Per donor, three control strips (polyurethane), three heparin-coated[33] strips, and three strips with the studied PEG-based coating were tested in a new ball valve model[34] through exposure to the heparinized whole human blood for 1 h at 37°C. During the incubation, blood recirculated pulsatile and unidirectionally through the tubing by means of an alternating movement at a flow rate of approximately 20 ml/min. Afterward, the samples were analyzed for fibrin binding and blood platelet adhesion (ISO 10993-4). Briefly, adhesion of fibrin was studied by determining the binding of a labeled antibody (specific to fibrin; almost no cross reaction with fibrinogen) to the surface of the incubated materials. The amount of adhered thrombocytes was assessed by measuring the activity of acid phosphatase, an enzyme present in platelet granules. In this determination, the incubated materials were exposed to citrate buffer with 4-nitrophenyl phosphate that was converted by the acid phosphatase from platelets. This resulted in a yellow color after alkalization, proportional to the amount of platelets, determined by UV spectrophotometry.

Determination of Glucose Permeability

This study was carried out at Cranfield Health.

A glucose meter from Roche (Accu-Chek Aviva) with corresponding testing strips was used.

Glucose transport through the coated membranes was determined for 4.4 and 6.6 mM glucose solutions. As controls, measurements were done in absence of any membrane and with uncoated cellulose acetate membranes. A membrane section was positioned in front of the glucose strip when inserted in the meter. An aliquot (5–10 μl) of glucose solution was pushed through the membrane using a pipette, and the amount of glucose reaching the strip was recorded.

Determination of Oxygen Permeability

This study was carried out at Cranfield Health.

A commercial oxygen electrode capable of measuring dissolved oxygen was purchased from Hanna Instruments (United Kingdom).

The oxygen probe was immersed in PBS solution, which was purged with nitrogen until a reading of 0% oxygen was obtained. Then, after a further 2 min of nitrogen purging, the nitrogen flow was stopped, and the diffusion of the atmospheric oxygen into the PBS solution was recorded using the oxygen meter every 10 s for 30 min under stirring.

The experiment was then repeated by wrapping uncoated cellulose acetate membranes with porosity 0.22, 0.65, or 1.2 μm around the tip of the oxygen probe. All oxygen was removed from the testing solution by nitrogen purging. The nitrogen flow was then stopped, and the diffusion of the atmospheric oxygen was measured every 10 s for 30 min under stirring.

The experiments were then repeated with the same type of cellulose acetate membranes containing coating applied from formulations of different solid contents (3.5 and 7.0 w%).

Results

Coating Thickness

Table 1 displays the thickness of coatings applied to the PET sheets and silicon wafers as determined by spectral reflectance measurements.

Optical Appearance

The coated PET sheets looked homogeneous and transparent. No coating defects were observed.

Mechanical Properties

As shown in **Table 2**, the coating adheres well to PET sheets under dry and wet conditions. The coating shows good integrity, scratch resistance, and flexibility.

Hydrophilicity

Figure 1 illustrates the different behavior of a water droplet when brought in contact with an uncoated and coated PET sheet.

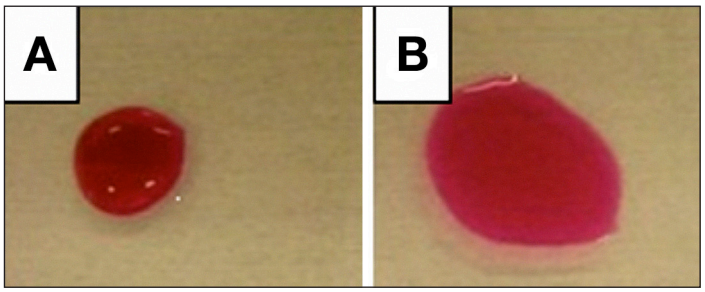

Figure 1. A water droplet, containing some Rhodamine B to improve visibility, was applied to **(A)** an uncoated PET sheet and **(B)** a coated PET sheet.

Table 1.
Thickness of Coatings Applied to Polyethylene Terephthalate Sheets and Silicon Wafers, Both $n = 3$, as Determined by Spectral Reflectance Measurements

Sample	Coating thickness (nm)
Coated PET sheet	175 ± 25
Coated silicon wafer	67 ± 7

Table 2.
Coating Cohesion and Adhesion between Coating and Substrate under Dry Conditions as Determined in the Cross-Hatching Test, Adhesion between the Coating and the Substrate under Wet Conditions Evaluated in the Wet Paper Rubbing Test, Coating Cohesion under Wet Conditions Analyzed in the Paper Double Rubbing Test, and Coating Flexibility Indicated as the Degree of Crack Formation in the Bending Test[a]

Test method	Result
Cross-hatching test	ASTM Class 5B
Wet paper rubbing test	No coating removal
Paper double rubbing test	No scratching, no coating removal
Bending test	No coating cracks

[a] All experiments were performed three times.

When water was applied to an uncoated PET sheet, no spreading of the water droplet was observed (**Figure 1A**). On the contrary, after applying the coating to the PET sheet, water spread over the coating, resulting in a wet spot 7–8 mm in diameter (n = 3; **Figure 1B**).

Lysozyme Adsorption

Table 3 shows that the application of the coating significantly reduces lysozyme adsorption to the silicon wafer. Furthermore, lysozyme adsorption to the coating is predominantly reversible in nature.

Bovine Serum Albumin Adsorption

More than 90% ± 8% reduction in BSA adsorption was found for coated tubes compared with uncoated tubes (both n = 10).

Biocompatibility–Hemocompatibility

Biocompatibility testing showed that the coating is not cytotoxic, demonstrating scores of zero in various tests. The coating is not expected to cause sensitization, irritation, or hemolysis.

Table 3.
Lysozyme Adsorption to Uncoated and to Coated Silicon Wafers[a]

Sample	A1 (mg/m^2)	A2 (mg/m^2)
Uncoated silicon wafer (n = 3)	>2	>2
Coated silicon wafer—sample 1	0.15	0.05
Coated silicon wafer—sample 2	0.12	0.01

[a] A1, protein adsorption after switching from PBS to lysozyme solution; A2, irreversible protein adsorption detected after switching back from lysozyme to PBS solution.

Furthermore, fibrin binding, as assessed as the binding of a labeled antibody, is very low. Only 10^{-6}% of total antibody was adhered to the different materials studied (**Figure 2**).

As shown in **Figure 3**, both the heparin and the PEG-based coating showed a large reduction in platelet adhesion as compared with the uncoated polyurethane. No difference was found between the heparin and the PEG-based coating.

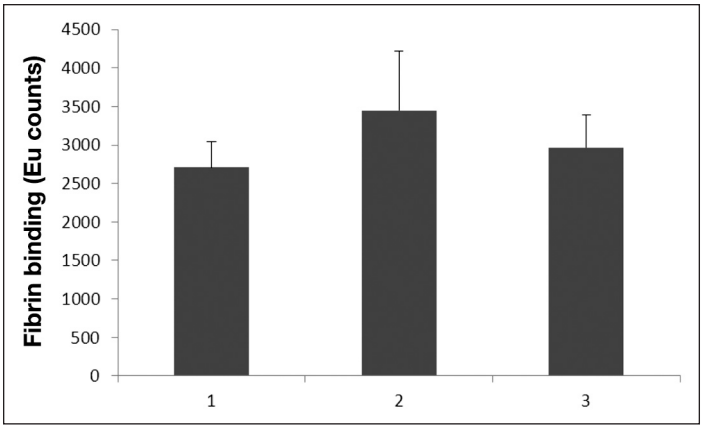

Figure 2. Fibrin binding to **(1)** uncoated polyurethane strips, **(2)** heparin-coated PET strips, and **(3)** coated PET strips containing the PEG-based coating under investigation, as assessed by binding of a Europium-labeled antibody to human fibrin. Fibrin binding is expressed by a fluorescence count. Data represent mean + standard deviation.

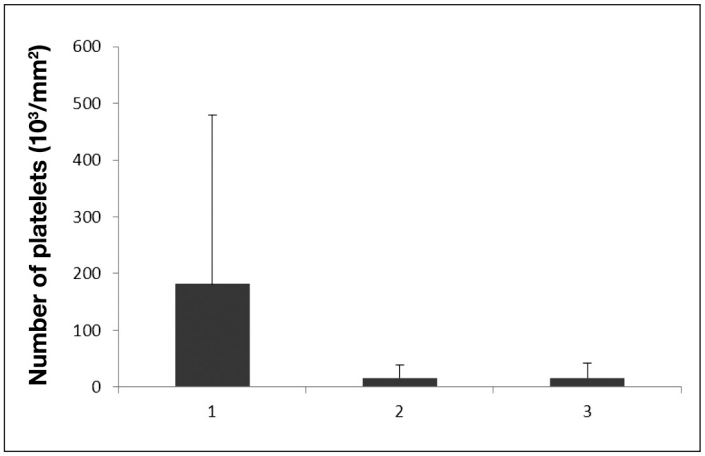

Figure 3. Platelet binding to **(1)** uncoated polyurethane strips, **(2)** heparin-coated PET strips, and **(3)** coated PET strips containing the PEG-based coating under investigation, as assessed by acid phosphatase release. Data were normalized for surface area and represent mean + standard deviation.

Coating Stability

The studied coating was applied to PET sheets and incubated in PBS solution at 37°C. After 1, 10, 20, and 30 days of incubation, coatings were evaluated for coating adhesion to the substrate, coating integrity, and coating flexibility. None of these characteristics were changed by incubation of the coated sheets in PBS solution up to 30 days.

Coating stability was further evaluated by measuring BSA adsorption to the coated PET tubes that contained PBS solution at 37°C for one and seven days. This incubation did not alter resistance to BSA adsorption.

Glucose Permeability

Results showed that the presence of the coating did not interfere with the transport of glucose through the membranes regardless of the intrinsic porosity of the membrane. In fact, no significant differences in glucose amount were observed when measuring with coated or uncoated membranes or in the absence of any membrane. **Figure 4** illustrates this for the membrane with lowest intrinsic porosity.

Oxygen Permeability

The investigation showed that the presence of membranes wrapped around the tip of the electrode slowed oxygen readings. This is not surprising as these membranes contain small pores that make physical diffusion harder. No significant differences in oxygen diffusion were observed among the three membrane porosities tested.

Figure 5 shows that oxygen permeability was approximately 30% lower for the membranes with a porosity of 0.22 μm and coated with the 7 w% coating formulation. On the other hand, the coating applied from the 3.5 w% coating formulation did not significantly affect oxygen diffusion, showing that a lower amount of coating does not interfere with the porosity of the membrane.

Oxygen diffusion through the membranes with higher porosity was not affected by the presence of the coatings studied.

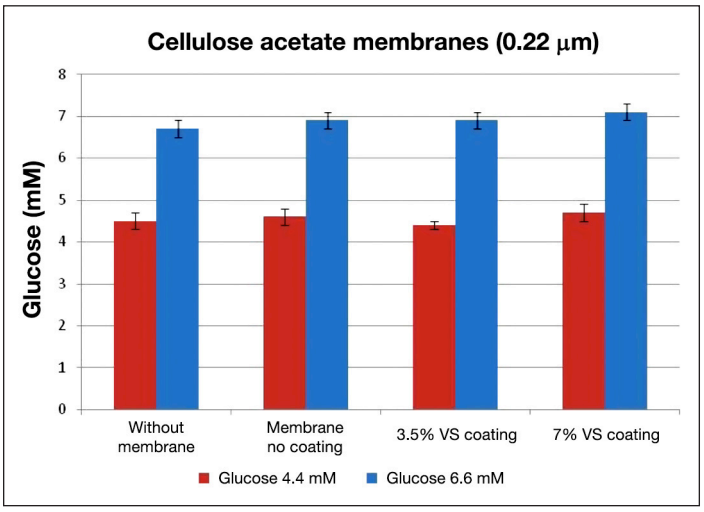

Figure 4. Glucose concentrations read by the Accu-Chek glucose meter in presence of 0.22 μm cellulose acetate membranes with and without coating. The data obtained in absence of any membrane are also shown. x% VS coating: membrane coated with x w% PEG-based coating formulation.

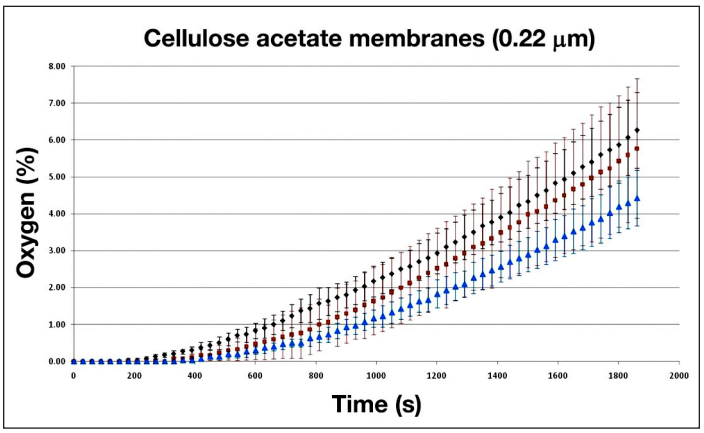

Figure 5. Diffusion of oxygen through uncoated and coated cellulose acetate membranes with porosity of 0.22 μm. Standard deviations were calculated for experiments performed with three different membranes of each type. (♦) uncoated membrane; membrane coated with respectively (■) 3.5 w% and (▲) 7 w% PEG-based coating formulation.

Discussion

As used in the study, the developed PEG-based coating appeared to be transparent, homogeneous, and free of defects. The coating showed good adhesion onto various substrates and good coating integrity and scratch resistance under dry and wet conditions. It was also possible to bend the coating without cracks forming. Stability testing showed that the properties mentioned earlier were maintained after incubation in PBS solution at 37°C for 30 days. The antifouling properties against BSA were evaluated after 7 days, and no changes were observed compared with a fresh coating.

The coating is hydrophilic in nature. Its brush structure reduces lysozyme adsorption to silicon wafers, BSA adsorption to PET tubes, and fibrin binding (compared with silicone; data not shown) and platelet binding to medical-grade polyurethane (comparable to heparin coating).

Cytotoxicity, irritation, sensitization, and hemolysis were assessed for coated PET sheets. Scores of zero in the various tests suggest good biocompatibility.

To ensure proper functionality, the unblocked flow of glucose and oxygen to CGM sensors is essential. This testing highlights that coatings applied from 3.5 and 7 w% formulations on cellulose acetate membranes do not affect the transport of glucose through membranes. Experiments performed to evaluate the transport of oxygen showed that the coating applied from the 7 w% formulation had a minimal effect on the performance of membranes with the smallest porosity (0.22 μm). The presence of a higher amount of coating slowed the flow rate of oxygen through the membrane by approximately 30%. No significant effect of the two coating formulations was observed for the other two types of membranes with porosities of 0.65 and 1.2 μm.

Conclusion

The developed PEG-based coating is characterized by good mechanical properties and strong coating stability under dry and wet conditions. The coating is hydrophilic in nature, and its brush structure repels the adsorption of lysozyme and BSA as well as of fibrin and blood platelets in whole human blood to a very large extent. Initial biocompatibility testing shows good results. The coating can be applied to the described cellulose acetate membranes without changing their permeability for glucose and oxygen. It thus can be concluded that the studied coating is a good candidate for further evaluation of its utility to improve the biostability of CGM sensors.

Funding:

This work was supported by Royal DSM N.V.

Disclosures:

The authors are employees of DSM Biomedical, a division of Royal DSM N.V.

Acknowledgments:

The authors thank HaemoScan (The Netherlands) and Cranfield Health (Scotland) for their valuable contributions.

References:

1. Halimi S. Acute consequences of hypoglycaemia in diabetic patients. Diabetes Metab. 2010;36 Suppl 3:S75–83.
2. Bonds DE, Miller ME, Dudl J, Feinglos M, Ismail-Beigi F, Malozowski S, Seaquist E, Simmons DL, Sood A. Severe hypoglycemia symptoms, antecedent behaviors, immediate consequences and association with glycemia medication usage: secondary analysis of the ACCORD clinical trial data. BMC Endocr Disord. 2012;12:5.
3. Boussageon R, Bejan-Angoulvant T, Saadatian-Elahi M, Lafont S, Bergeonneau C, Kassaï B, Erpeldinger S, Wright JM, Gueyffier F, Cornu C. Effect of intensive glucose lowering treatment on all cause mortality, cardiovascular death, and microvascular events in type 2 diabetes: meta-analysis of randomised controlled trials. BMJ. 2011;343:d4169.
4. Wentholt IM, Vollebregt MA, Hart AA, Hoekstra JB, DeVries JH. Comparison of a needle-type and a microdialysis continuous glucose monitor in type 1 diabetic patients. Diabetes Care. 2005;28(12):2871–6.
5. Wickramasinghe Y, Yang Y, Spencer SA. Current problems and potential techniques in *in vivo* glucose monitoring. J Fluoresc. 2004;14(5):513–20.
6. Abel PU, von Woedtke T. Biosensors for *in vivo* glucose measurement: can we cross the experimental stage. Biosens Bioelectron. 2002;17(11-12):1059–70.
7. Heinemann L, Koschinsky T. Continuous glucose monitoring: an overview of today's technologies and their clinical applications. Int J Clin Pract Suppl. 2002;129:75–9.
8. Sieg A, Guy RH, Delgado-Charro MB. Noninvasive and minimally invasive methods for transdermal glucose monitoring. Diabetes Technol Ther. 2005;7(1):174–97.
9. Pickup J, Rolinski O, Birch D. *In vivo* glucose sensing for diabetes management: progress towards non-invasive monitoring. Interview by Judy Jones. BMJ. 1999;319(7220):1289.
10. Wilson GS, Gifford R. Biosensors for real-time *in vivo* measurements. Biosens Bioelectron. 2005;20(12):2388–403.
11. Cardosi MF, Birch SW. Screen printed glucose electrodes based on platinised carbon particles and glucose oxidase. Anal Chim Acta. 1993;276:69–74.
12. Mizutani F, Yabuki S, Iijima S. Carbon paste electrode incorporated with cobalt(II) octaethoxyphthalocyanine for the amperometric detection of hydrogen peroxide. Electroanalysis. 1995;7(8):706–9.
13. Fischer U. Continuous *in vivo* monitoring in diabetes: the subcutaneous glucose concentration. Acta Anaesthesiol Scand Suppl. 1995;104:21–9.

14. Fischer U, Ertle R, Abel P, Rebrin K, Brunstein E, Hahn von Dorsche H, Freyse EJ. Assessment of subcutaneous glucose concentration: validation of the wick technique as a reference for implanted electrochemical sensors in normal and diabetic dogs. Diabetologia. 1987;30(12):940–5.

15. Pickup JC, Shaw GW, Claremont DJ. *In vivo* molecular sensing in diabetes mellitus: an implantable glucose sensor with direct electron transfer. Diabetologia. 1989;32(3):213–7.

16. Moussy F, Harrison DJ, Rajotte RV. A miniaturized Nafion-based glucose sensor: *in vitro* and *in vivo* evaluation in dogs. Int J Artif Organs. 1994;17(2):88–94.

17. Claremont DJ, Sambrook IE, Penton C, Pickup JC. Subcutaneous implantation of a ferrocene-mediated glucose sensor in pigs. Diabetologia. 1986;29(11):817–21.

18. Steil GM, Rebrin K, Mastrototaro J, Bernaba B, Saad MF. Determination of plasma glucose during rapid glucose excursions with a subcutaneous glucose sensor. Diabetes Technol Ther. 2003;5(1):27–31.

19. Rebrin K, Fischer U, Hahn von Dorsche H, von Woetke T, Abel P, Brunstein E. Subcutaneous glucose monitoring by means of electrochemical sensors: fiction or reality. J Biomed Eng. 1992;14(1):33–40.

20. Cote GL, Lec RM, Pishko MV. Emerging biomedical sensing technologies and their applications. IEEE Sens J. 2003;3(3):251–66.

21. Pickup JC. *In vivo* glucose monitoring: sense and sensorbility. Diabetes Care. 1993;16(2):535–9.

22. Pfeiffer EF. On the way to the automated (blood) glucose regulation in diabetes: the dark past, the grey present and the rosy future. XII Congress of the International Diabetes Federation, Madrid, 22-28 September 1985. Diabetologia. 1987;30(2):51–65.

23. Valdes TI, Moussy F. *In vitro* and *in vivo* degradation of glucose oxidase enzyme used for an implantable glucose biosensor. Diabetes Technol Ther. 2000;2(3):367–76.

24. Kvist PH, Iburg T, Bielecki M, Gerstenberg M, Buch-Rasmussen T, Hasselager E, Jensen HE. Biocompatibility of electrochemical glucose sensors implanted in the subcutis of pigs. Diabetes Technol Ther. 2006;8(4):463–75.

25. Tang L, Eaton JW. Fibrin(ogen) mediates acute inflammatory responses to biomaterials. J Exp Med. 1993;178(6):2147–56.

26. Maitra M, Abbas AK. The endocrine system. In: Kumar V, Abbas AK, Fausto N, eds. Robbins and Cotran pathologic basis of disease. Philadelphia: Elsevier Saunders; 2005, 1189–205.

27. Wang YX, Robertson JL, Spillman WB Jr, Claus RO. Effects of the chemical structure and the surface properties of polymeric biomaterials on their biocompatibility. Pharm Res. 2004;21(8):1362–73.

28. Kvist PH, Jensen HE. Recent advances in continuous glucose monitoring: biocompatibility of glucose sensors for implantation in subcutis. J Diabetes Sci Technol. 2007;1(5):746–52.

29. Tang L, Eaton JW. Inflammatory responses to biomaterials. Am J Clin Pathol. 1995;103(4):466–71.

30. Klueh U, Liu Z, Feldman B, Henning TP, Cho B, Ouyang T, Kreutzer D. Metabolic biofouling of glucose sensors *in vivo*: role of tissue microhemorrhages. J Diabetes Sci Technol. 2011;5(3):583–95.

31. Holmes PF, Currie EP, Thies JC, Van der Mei HC, Busscher HJ, Norde W. Surface-modified nanoparticles as a new, versatile, and mechanically robust nonadhesive coating: Suppression of protein adsorption and bacterial adhesion. J Biomed Mater Res A. 2009;91(3):824–33.

32. Dijt JC, Stuart MA, Hofman JE, Fleer GJ. Kinetics of polymer adsorption in stagnation point flow. Coll Surf. 1990;51:141–58.

33. Tan Q, Ji J, Barbosa MA, Fonseca C, Shen J. Constructing thromboresistant surface on biomedical stainless steel via layer-by-layer deposition anticoagulant. Biomaterials. 2003;24(25):4699–705.

34. Van Oeveren W, Tielliu IF, de Hart J. Comparison of modified Chandler, roller pump, and ball valve circulation models for *in vitro* testing in high blood flow conditions: application in thrombogenicity testing of different materials for vascular applications. Int J Biomater. 2012;2012:673163.